Neurobiology of Aging xxx (2020) 1–11

Contents lists available at ScienceDirect

Neurobiology of Aging

journal homepage: www.elsevier.com/locate/neuaging

In vivo staging of regional amyloid deposition predicts functional conversion in the preclinical and prodromal phases of Alzheimer's disease

Stefan J. Teipel[a,b,*], Martin Dyrba[a], Patrizia A. Chiesa[c,d,e], Fatemah Sakr[b], Irina Jelistratova[a], Simone Lista[c,d,e], Andrea Vergallo[c], Pablo Lemercier[c,d,e], Enrica Cavedo[c,d,e,f], Marie Odile Habert[g,h,i], Bruno Dubois[e], Harald Hampel[c], Michel J. Grothe[a,j], the INSIGHT-preAD study group and for the Alzheimerś Disease Neuroimaging Initiative[*]

[a] German Center for Neurodegenerative Diseases (DZNE), Rostock, Germany
[b] Department of Psychosomatic Medicine, University Medicine Rostock, Rostock, Germany
[c] Sorbonne University, GRC n° 21, Alzheimer Precision Medicine (APM), AP-HP, Pitié-Salpêtrière Hospital, Boulevard de l'hôpital, Paris, France
[d] Brain & Spine Institute (ICM), INSERM U 1127, CNRS UMR 7225, Boulevard de l'hôpital, Paris, France
[e] Institute of Memory and Alzheimer's Disease (IM2A), Department of Neurology, Pitié-Salpêtrière Hospital, AP-HP, Boulevard de l'hôpital, Paris, France
[f] Qynapse, Paris, France
[g] Sorbonne University, CNRS, INSERM, Laboratoire d'Imagerie Biomédicale, LIB, Paris, France
[h] AP-HP, Pitié-Salpêtrière Hospital, Department of Nuclear Medicine, Paris, France
[i] Centre d'Acquisition et Traitement des Images (CATI Platform), Paris, France
[j] Unidad de Trastornos del Movimiento, Servicio de Neurología y Neurofisiología Clínica, Instituto de Biomedicina de Sevilla, Hospital Universitario Virgen del Rocío/CSIC/Universidad de Sevilla, Seville, Spain

ARTICLE INFO

Article history:
Received 13 September 2019
Received in revised form 10 March 2020
Accepted 12 March 2020

Keywords:
Amyloid
Longitudinal study
Dementia
MCI
Subjective cognitive decline

ABSTRACT

We tested the usefulness of a regional amyloid staging based on amyloid sensitive positron emission tomography to predict conversion to cognitive impairment and dementia in preclinical and prodromal Alzheimer's disease (AD). We analyzed 884 cases, including normal controls, and people with subjective cognitive decline or mild cognitive impairment (MCI), from the Alzheimer's Disease Neuroimaging Initiative with a maximum follow-up of 6 years and 318 cases with subjective memory complaints with a maximum follow-up time of three years from the INveStIGation of AlzHeimer's PredicTors cohort (INSIGHT-preAD study). Cox regression showed a significant association of regional amyloid stages with time to conversion from a cognitively normal to an MCI, and from an MCI to a dementia status. The most advanced amyloid stages identified very-high-risk groups of conversion. All results were robustly replicated across the independent samples. These findings indicate the usefulness of regional amyloid staging for identifying preclinical and prodromal AD cases at very high risk of conversion for future amyloid targeted trials.

1. Introduction

Cerebral amyloid deposition is considered an upstream event in the pathogenesis of Alzheimer's disease (AD) (Thal et al., 2006). In vivo imaging using amyloid sensitive positron emission tomography (PET) detected increased levels of amyloid in 15%–30% of cognitively normal people older than 70 years, and in at least 50% of people with a clinical phenotype of amnestic mild cognitive impairment (MCI) (Quigley et al., 2010). However, the positive predictive value of increased amyloid signal in PET for subsequent cognitive decline in preclinical or prodromal AD cases is limited. In

* Corresponding author at: Department of Psychosomatic Medicine, University Medicine Rostock, and DZNE Rostock, Gehlsheimer Str. 20, 18147 Rostock, Germany. Tel.: +1149 381 494 9470; fax: +1149 381 494 9682.
E-mail address: stefan.teipel@med.uni-rostock.de (S.J. Teipel).

* Data used in preparation of this article were obtained from the Alzheimer's Disease Neuroimaging Initiative (ADNI) database (adni.loni.usc.edu/). As such, the investigators within the ADNI contributed to the design and implementation of ADNI and/or provided data but did not participate in analysis or writing of this report. A complete listing of ADNI investigators can be found at: http://adni.loni.usc.edu/wp-content/uploads/how_to_apply/ADNI_Acknowledgement_List.pdf.

0197-4580/$ – see front matter © 2020 Elsevier Inc. All rights reserved.
https://doi.org/10.1016/j.neurobiolaging.2020.03.011

cognitively normal people, the positive predictive value of a positive amyloid PET status for subsequent conversion to MCI or dementia is only about 25% over 3–5 years of follow-up (Baker et al., 2017; Morris et al., 2009; Villemagne et al., 2011). In people with MCI, the positive predictive value of positive amyloid status for subsequent conversion to AD dementia is about 65%–84% for a follow-up period of 3–5 years (Martinez et al., 2017; Zhang et al., 2014).

The current standard of amyloid PET imaging data analysis is a dichotomous classification in amyloid-positive or amyloid-negative cases (Klunk et al., 2015). Recently, we have developed a more fine-grained (Grothe et al., 2017) and replicable (Sakr et al., 2019) PET-based in vivo amyloid staging scheme that considers five regional stages of progressive cerebral amyloid deposition. The staging identified neurobiologically meaningful regional variation of amyloid deposition even in people with an amyloid-negative status, as shown by associations of amyloid stages with cerebrospinal fluid (CSF) Aβ1-42 concentrations and cognitive performance. An alternative tripartite staging approach has been based on differential involvement of cortical versus subcortical structures (amygdala, putamen, and caudate nucleus) (Cho et al., 2018). This previous study showed promising results for the predictive utility of amyloid staging but lacked a differentiation of cortical stages and a comparison with the standard binary classification.

Here, we evaluated the usefulness of regional amyloid staging to predict conversion of cognitively normal people with and without subjective cognitive decline (SCD) or subjective memory complaints (SMC) to MCI or AD dementia and of MCI cases to AD dementia, respectively. We compared our results with classical binary amyloid classification. We studied replicability of effects in three different longitudinal samples: a sample from the Alzheimer's Disease Neuroimaging Initiative (ADNI) that had previously been used for establishing the regional amyloid staging approach (Grothe et al., 2017), a second sample from ADNI that was not part of the development of the staging scheme, and an independent cohort of SMC cases from the monocentric INveStIGation of AlzHeimer's PredicTors in subjective memory complainers (INSIGHT-preAD) cohort (Dubois et al., 2018). As an endpoint, we assessed functional conversion as defined by transition in clinical dementia rating scale (CDR) scores (Berg, 1988).

2. Materials and methods

2.1. Data source

Data used in the preparation of this article were obtained from two independent cohorts. The first cohort contained data from the ADNI database (http://adni.loni.usc.edu/). The ADNI was launched in 2003 by the National Institute on Aging, the National Institute of Biomedical Imaging and Bioengineering, the Food and Drug Administration, private pharmaceutical companies, and nonprofit organizations, with the primary goal of testing whether neuroimaging, neuropsychologic, and other biologic measurements can be used as reliable in vivo markers of AD pathogenesis. A fuller description of ADNI and up-to-date information is available at www.adni-info.org. The second cohort was taken from the INSIGHT-preAD study (Dubois et al., 2018). The INSIGHT-preAD study is a monocentric university-based cohort derived from the Institute for Memory and Alzheimer's Disease at the Pitié-Salpêtrière University Hospital in Paris, France, that aims to investigate the earliest preclinical stages of AD and its development including influencing factors and markers of progression.

2.2. Study participants

From the ADNI cohort, we retrieved two different samples: first, a sample of 582 cases that was previously used to establish the regional amyloid staging approach (Grothe et al., 2017), henceforth termed ADNI-A sample, and second an independent sample of 302 cases that had not been part of the previous analysis, henceforth termed ADNI-B sample. Both samples provided amyloid PET data at baseline as well as longitudinal clinical follow-up using cognitive testing over a maximum interval of 6 years. ADNI-A included data of 179 cognitively normal elderly subjects, and 403 subjects with MCI. Mean follow-up time was 3.3 (SD 1.8) years. ADNI-B included data of 75 cognitively normal older subjects, 103 subjects with SCD, and 124 subjects with MCI. Mean follow-up time was 3.2 (SD 1.8) years. Detailed inclusion criteria for the diagnostic categories can be found at the ADNI web site (http://adni.loni.usc.edu/methods/).

The INSIGHT-preAD study included 318 cognitively normal Caucasian individuals from the Paris area at the baseline, between 70 and 85 years old, with subjective memory complaints and with defined brain amyloid status (Dubois et al., 2018). The study aims at a total of 7 years of annual follow-up, with the first three years follow-up being available for the current analysis; the mean follow-up time was 2.7 (SD 0.8) years. Details on participants' demographics for the 3 samples are shown in Table 1.

All procedures performed in the ADNI studies and the INSIGHT-preAD study involving human participants were in accordance with the ethical standards of the institutional research committees and with the 1975 Helsinki declaration and its later amendments. Written informed consent was obtained from all participants and/or authorized representatives and the study partners before any protocol-specific procedures were carried out in the ADNI or INSIGHT-preAD studies, respectively.

Table 1
Participant's demographics

Cohorts/Diagnoses	m/f	Age (SD) [years]	MMSE (SD)	Non-stageable	Median follow-up [months] (interquartile range)
ADNI-A					
Controls	88/91	73.8 (6.5)	29.1 (1.2)	3 (1.7%)	65 (54; 68)
MCI	220/183	71.8 (7.6)	28.1 (1.7)	4 (0.7%)	47 (43; 51)
ADNI-B					
Controls	36/39	79.2 (5.2)	29.2 (1.3)	1 (1.3%)	64 (60; 71)
MCI	79/45	75.4 (8.1)	27.8 (1.8)	3 (2.4%)	52 (49; 56)
SCD	42/61	72.4 (5.6)	29.0 (1.2)	4 (3.9%)	51 (38; 59)
INSIGHT-preAD					
SMC	114/204	76.5 (3.5)	28.7 (1.0)	2 (0.6%)	Non estimable[a]

Key: MMSE, Mini-Mental State Examination;SCD, subjective cognitive decline according to the definition in the ADNI cohort (Risacher et al., 2015) SMC, subjective memory complaints as defined in the INSIGHT-preAD cohort (Dubois et al., 2018).

[a] The proportion of censoring in the reversed survival plot with censored data assigned as events did not reach the median value during the available observation time.

2.2.1. Cognitive tests

Both ADNI and INSIGHT-preAD cohorts underwent comprehensive neuropsychological examinations at least every 12 months. The Mini-Mental State Examination (Folstein et al., 1975) was available for both cohorts to assess global cognition. We used the CDR score (Berg, 1988) as primary endpoint to assess change in functional status.

2.2.2. Imaging data acquisition

Detailed acquisition and standardized preprocessing steps of ADNI imaging data are available at the ADNI website (https://adni.loni.usc.edu/methods/). Amyloid-PET data were collected during a 50- to 70-minute interval following a 370 MBq bolus injection of 18F-Florbetapir. To account for the multicentric acquisition of the data across different scanners and sites, all PET scans undergo standardized preprocessing steps within ADNI.

The methods and results for the PET data acquisition in the INSIGHT-preAD cohort have been detailed in a previous paper (Habert et al., 2017). All amyloid PET scans were acquired in a single session on a Philips Gemini GXL CT-PET scanner 50 (±5) minutes after the injection of approximately 370 MBq (333–407 MBq) of 18F-Florbetapir (AVID radiopharmaceuticals).

For anatomical reference and preprocessing of the PET scans we used the corresponding structural MRI scan that was closest in time to the Florbetapir PET scan. In the ADNI-A sample, MRI data were acquired on multiple 3T MRI scanners using scanner-specific T1-weighted sagittal 3D MPRAGE sequences. The ADNI-B sample additionally included 1.5 T MRI scans from 155 cases. Similar to the PET data, MRI scans undergo standardized preprocessing steps aimed at increasing data uniformity across the multicenter scanner platforms (see https://adni.loni.usc.edu/methods/for detailed information on multicentric MRI acquisition and preprocessing in ADNI). MRI scans for INSIGHT-preAD were acquired on a Siemens Verio 3T scanner at Pitié-Salpêtrière Hospital, Paris. A T1-weighted image was acquired using a fast 3-dimensional gradient echo pulse sequence using a magnetization preparation pulse (Turbo FLASH) (Habert et al., 2017).

2.2.3. Imaging data preprocessing

Images were preprocessed using Statistical Parametric Mapping software version 8 (SPM8) (The Wellcome Trust Centre for Neuroimaging, Institute of Neurology, University College London) implemented in MATLAB 2013. The preprocessing pipeline followed the routine previously described in the study by Grothe et al., 2017. First, each subject's averaged PET frames were coregistered to their corresponding T1-weighted MRI scan. Then, partial volume effects (PVE) were corrected in native space using the 3-compartmental voxel-based postreconstruction method as described by Müller-Gärtner and colleagues (Gonzalez-Escamilla et al., 2017; Müller-Gärtner et al., 1992). The corrected PET images were spatially normalized to an aging/AD-specific reference template using the deformation parameters derived from the normalization of their corresponding MRI.

The regional 18F-Florbetapir–PET mean uptake values were estimated for 52 brain regions defined by the Harvard–Oxford structural atlas (Desikan et al., 2006), including both cortical and subcortical regions (https://fsl.fmrib.ox.ac.uk/fsl/fslwiki/Atlases). Standard uptake value ratios ($SUVR_{Cer}$) were computed for the 52 brain regions by dividing the mean uptake values by the mean uptake value of the whole cerebellum as estimated in non–PVE-corrected PET data (Catafau et al., 2016; Gonzalez-Escamilla et al., 2017; Grothe et al., 2017; Klunk et al., 2015).

In accordance with the methods used for the published PET-based amyloid staging approach, we based the cutoff used for determining regional amyloid positivity on a cutoff value of $SUVR_{Cer} = 1.135$ (Grothe et al., 2017), which lies in between the 2 most widely used global signal cutoffs for non–PVE-corrected 18F-Florbetapir-PET SUVRs, that is, $SUVR_{Cer} = 1.10$ (Clark et al., 2012; Joshi et al., 2012; Landau et al., 2013) and $SUVR_{Cer} = 1.17$ (Clark et al., 2011a; Fleisher et al., 2011). This threshold was converted to the PVE-corrected PET data used for the regional staging approach using linear regression between PVE-corrected and noncorrected global $SUVR_{Cer}$ values, which resulted in a value of $SUVR_{Cer} = 0.92$ in the ADNI cohort (Grothe et al., 2017) and of $SUVR_{Cer} = 0.98$ in the INSIGHT-preAD cohort (Sakr et al., 2019).

2.2.4. PET data analysis

Staging of regional amyloid deposition followed the previously developed 4-stage model of amyloid pathology progression derived from 18F-Florbetapir-PET data of cognitively normal older individuals enrolled in the ADNI study (Grothe et al., 2017). This 4-stage model was estimated by counting the frequency of amyloid positivity across the 52 brain regions defined in the Harvard–Oxford structural atlas and then merging the regions into 4 broader anatomical divisions based on equal proportions of the observed range of involvement frequencies. The 4 anatomical divisions defining the staging scheme are illustrated in Fig. 1.

According to this staging approach (Grothe et al., 2017), an anatomical division was considered positive for amyloid pathology if at least 50% of the regions included in this division exceeded the cutoff value in the respective participant. Subsequently, participants were classified as stage I if only the first division was considered positive. Then, the successive stages II-IV were defined by the additional involvement of their corresponding divisions II, III, and IV, respectively. Participants who exhibited amyloid positivity in any division without concurrent amyloid positivity in the preceding divisions were classified as nonstageable (mismatch).

For comparison, we also studied conventional classifications of 18F-Florbetapir–PET scans into global amyloid-positive or amyloid-negative categories. For the ADNI data, this classification was derived using centrally calculated global composite $SUVR_{Cer}$ values that are made available on the ADNI server (Jagust Lab, UC Berkley; adni.loni.usc.edu/methods/pet-analysis). Originally, amyloid positivity was defined using a cutoff of $SUVR_{Cer} > 1.17$ (Clark et al., 2011a; Fleisher et al., 2011). The even more widely recommended cutoff of $SUVR_{Cer} > 1.1$ (Clark et al., 2012; Joshi et al., 2012; Landau et al., 2013) yielded inferior results for the prediction accuracy so that we decided to use the better performing cutoff for the reference test of global amyloid status. For the INSIGHT-preAD data, the classification was based on centrally calculated global composite values published by the INSIGHT-preAD PET core, and amyloid positivity was defined using a recommended cutoff of 0.88 for this data, which resulted from a conversion of the aforementioned cutoff of $SUVR_{Cer} > 1.1$ to the specific processing pipeline used by the INSIGHT-preAD PET core (Habert et al., 2018). A lower cutoff of SUVR >0.79 that was also published by the INSIGHT-preAD PET core yielded lower prediction performance in our analyses so that again we decided to use the better performing cutoff for the reference test.

2.2.5. Statistical analysis

We predicted time to conversion in CDR status (from 0 to 0.5 or higher, and from 0.5 to 1 or higher, respectively) using Cox regression with regional amyloid stages, age, and sex as predictors taking censoring into account. For comparison, we replaced regional amyloid stages by binary amyloid status in the model. This analysis was conducted using the R library "survival" with the command "coxph" for Cox regression. We compared overall model fit as estimated from Akaike information criterion (AIC) between Cox regression models based on staging versus models based on

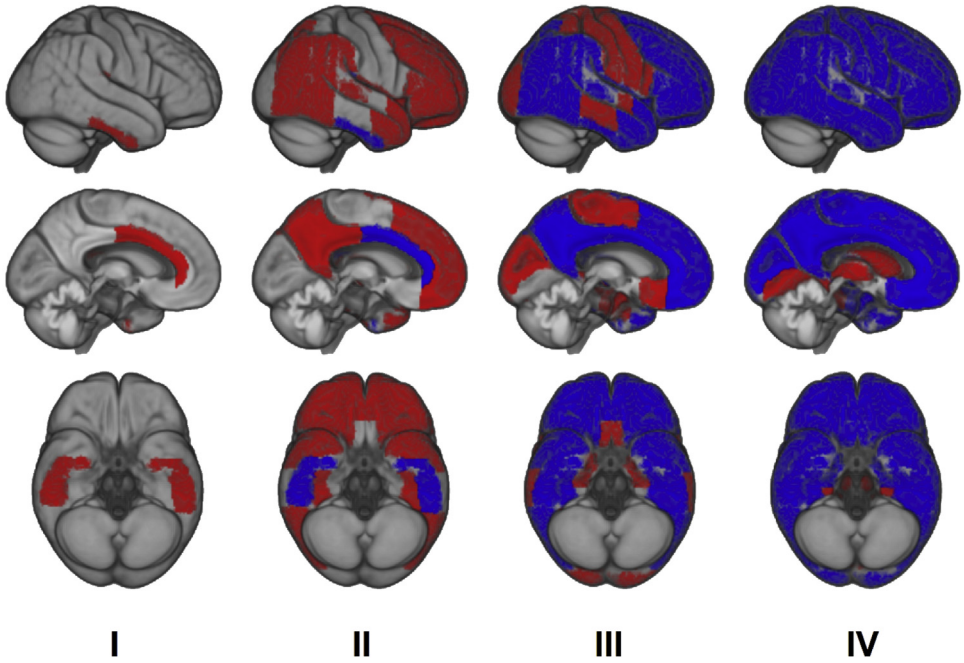

Fig. 1. Regional amyloid stages. Stages I to IV of nested regional amyloid accumulation, according to the previously established staging approach (Grothe et al., 2017). Adapted with permission from the previous publication (Grothe et al., 2017).

global amyloid load. We selected the AIC as fit index as it penalizes the use of a higher number of parameters, hence discourages overfitting (Burnham and Anderson, 2004). In addition, we conducted survival curve analysis with regional amyloid stages as predictor, adjusted for average age and sex distribution within each stratum. For comparison, we replaced regional amyloid stages by binary amyloid status in the curve fitting. This analysis used the R library "survminer" with the command "survfit" for survival curve plotting. Analyses were performed with RStudio, version 1.1.463, a user interface of R Project for Statistical Computing Analyses. The libraries used are available at http://cran.r-project.org/web/packages.

3. Results

3.1. Staging

Across the 1202 cases, we found 17 cases (1.4%) that were nonstageable, that is, whose regional amyloid distribution violated the regional staging scheme depicted in Fig. 1. The distribution of nonstageable cases across cohorts and diagnoses is shown in Table 1. The subsequent analyses exclude these nonstageable cases.

The following results report hazard ratios (HRs) and 95% confidence intervals relative to stage 0 for the amyloid stages and relative to the amyloid-negative cases for the binary classification based on global amyloid.

3.2. ADNI-A sample

For prediction of CDR conversion in the cognitively normal controls, HR relative to stage 0 was 4.4 (95% confidence interval 1.7–11.6) for stage II and 4.8 (1.7–13.8) for stage IV, but there was no significant effect for stages I and III. For binary amyloid the HR was 3.1 (1.4–6.6) relative to amyloid-negative cases (see Table 2 for details). Correspondingly, the stage IV cases had 50% conversion compared with 35% conversion for global amyloid increase.

For prediction of CDR conversion in the MCI cases, we found significant effects for amyloid stage III with an HR of 7.0 (3.3–14.7), and stage IV with an HR of 9.6 (4.7–19.5). The prediction by global amyloid ($SUVR_{Cer} > 1.17$) was significant as well with an HR of 7.7 (4.1–14.4) (see Table 2 for details). Risk enrichment was strongest in the stage IV cases with 47% conversion compared with 38% for global amyloid increase (Fig. 2).

Both for controls and MCI cases, the lower cutoff for global amyloid of $SUVR_{Cer} > 1.1$ yielded inferior results.

3.3. ADNI-B sample

For prediction of CDR conversion, results were similar to those in the ADNI-A sample. In the MCI cases, HR was 18.0 (2.3–142.4) for stage III, and 27.1 (3.4–216.2) for stage IV, but there was no significant effect for stages I and II. For binary amyloid the HR was 23.5 (3.1–175.3) (see Table 2 for details). The stage III cases had 55% conversion and the stage IV cases 52% conversion, compared with 45% conversion for global amyloid increase (Fig. 3).

Only 2 cases of the cognitively normal controls were amyloid stage IV, so that we pooled amyloid stages III and IV (henceforth stage III/IV). For the cognitively normal controls, the HR was 4.1 (1.3–13.3) for stage II, and 8.7 (2.9–26.2) for stage III/IV. For binary amyloid the HR was 6.2 (2.5–15.6) (see Table 2 for details). The stage II cases had 55% conversion, and the stage III/IV cases 77%, compared with 65% conversion for global amyloid increase.

For the cases with SCD, the HR was 4.9 (1.4–17.3) for stage IV, but there was no significant effect for stages I through III. For binary amyloid, the HR was not significant (see Table 2 for details). The stage IV cases had 56% conversion, compared with 32% conversion for global amyloid increase.

3.4. Insight-preAD sample

For the INSIGHT-preAD SMC cases, only 4 cases were amyloid stage IV at the baseline, so that we pooled amyloid stages III and IV (henceforth stage III/IV).

Table 2
Results of Cox regression models

Cohort	Group	Amyloid status	Number of cases	HR (SE)	*p*	AIC	Median time to conversion [months]
ADNI-A	Controls	0	95	-	-	237	n.r.
		I	27	<0.1	n.s.		n.r.
		II	15	4.4 (0.49)	<0.003		70
		III	20	1.8 (0.60)	n.s.		n.r.
		IV	12	4.8 (0.54)	<0.004		66
		A−	132	-	-	260[b]	n.r.
		A+	40	3.1 (0.40)	<0.004		70
	MCI	0	136	-	-	790	n.r.
		I	34	0.7 (1.1)	n.s.		70
		II	44	1.6 (0.59)	n.s.		n.r.
		III	75	7.0 (0.38)	<0.0001		66
		IV	85	9.6 (0.36)	<0.0001		55
		A−	194	-	-	794[c]	n.r.
		A+	183	7.7 (0.32)	<0.0001		63
ADNI-B	Controls	0	37	-	-	173	n.r.
		I	9	1.3 (0.82)	n.s.		n.r.
		II	11	4.1 (0.60)	<0.02		37
		III/IV	13	8.7 (0.56)	<0.0002		35
		A−	48	-	-	170	n.r.
		A+	23	6.2 (0.47)	<0.0001		35
	MCI	0	39	-	-	173	n.r.
		I	11	<0.1	n.s.		n.r
		II	14	6.0 (1.2)	n.s.		63
		III	20	18.0 (1.06)	<0.007		36
		IV	21	27.1 (1.06)	<0.002		36
		A−	50	-	-	186[a]	n.r.
		A+	58	23.5 (1.03)	<0.003		63
	SCD	0	49	-	-	176	n.r.
		I	14	0.9 (0.81)	n.s.		n.r.
		II	11	1.1 (0.86)	n.s.		n.r.
		III	13	3.2 (0.62)	n.s.		n.r.
		IV	9	4.9 (0.64)	<0.02		50
		A−	62	-	-	193[a]	n.r.
		A+	37	1.9 (0.43)	n.s.		n.r.
INSIGHT-preAD	SMC	0	162	-	-	211	n.r.
		I	78	1.0 (0.64)	n.s.		n.r.
		II	40	0.48 (1.1)	n.s.		n.r.
		III/IV	36	5.5 (0.52)	<0.002		n.r.
		A−	255	-	-	214[d]	n.r.
		A+	63	3.2 (0.45)	<0.02		n.r.

SCD, subjective cognitive decline according to the definition in the ADNI cohort (Risacher et al., 2015).
SMC, subjective memory complaints as defined in the INSIGHT-preAD cohort (Dubois et al., 2018).
I–IV, amyloid stages.
A+, amyloid positive according to global threshold.
n.r., not reached.
Key: ADNI, Alzheimer's Disease Neuroimaging Initiative; AIC, Akaike information criterion; MCI, mild cognitive impairment; HR, hazard ratio with standard error (SE) from cox regression models, including age and sex as covariates.
[a] Probability $p < 0.002$ that the binary model minimizes AIC compared with the staging model.
[b] Probability $p < 0.0001$ that the binary model minimizes AIC compared with the staging model.
[c] Probability $p = 0.13$ that the binary model minimizes AIC compared with the staging model.
[d] Probability $p = 0.22$ that the binary model minimizes AIC compared with the staging model.

For prediction of CDR conversion in the INSIGHT-preAD SMC cases, we found significant effects for amyloid stage III/IV with an HR of 5.5 (1.8–15.2). The prediction by global amyloid ($SUVR_{Cer} > 0.88$) was significant as well with an HR of 3.2 (1.2–7.7) (see Table 2 for details). The lower cutoff for global amyloid of $SUVR_{Cer} > 0.79$ yielded inferior results. Risk enrichment was strongest in the stage III/IV cases with 22% conversion compared with 14% for global amyloid increase (Fig. 4).

3.5. Model fit

As reported in Table 2, for all except one comparison, the staging-based models had lower AIC than the global amyloid load–based model so that the staging-based models would be preferred. The probability for the global amyloid model to provide a better fit than the staging model was below 0.002 for the ADNI-A controls and the ADNI-B MCI and SCD cases, and below 0.3 for the ADNI-A MCI cases and the INSIGHT-preAD SMC cases. Only for the ADNI-B controls was the fit as measured by AIC better for the binary than the stage model.

4. Discussion

We found a significant association of regional amyloid stages and global amyloid status with time to conversion from a functionally healthy status to mild functional impairment and from mild functional impairment to dementia, respectively. These findings were widely consistent across the three independent samples.

The association of global amyloid status with change in functional status agrees with previous studies using amyloid sensitive PiB-PET as summarized in a meta-analysis covering controls and MCI cases (Chen et al., 2014) and replicated in subsequent studies on MCI cases (Frings et al., 2018; Iaccarino et al., 2017). Similar results were reported for amyloid sensitive ^{18}F tracers in MCI (Schreiber et al., 2015),

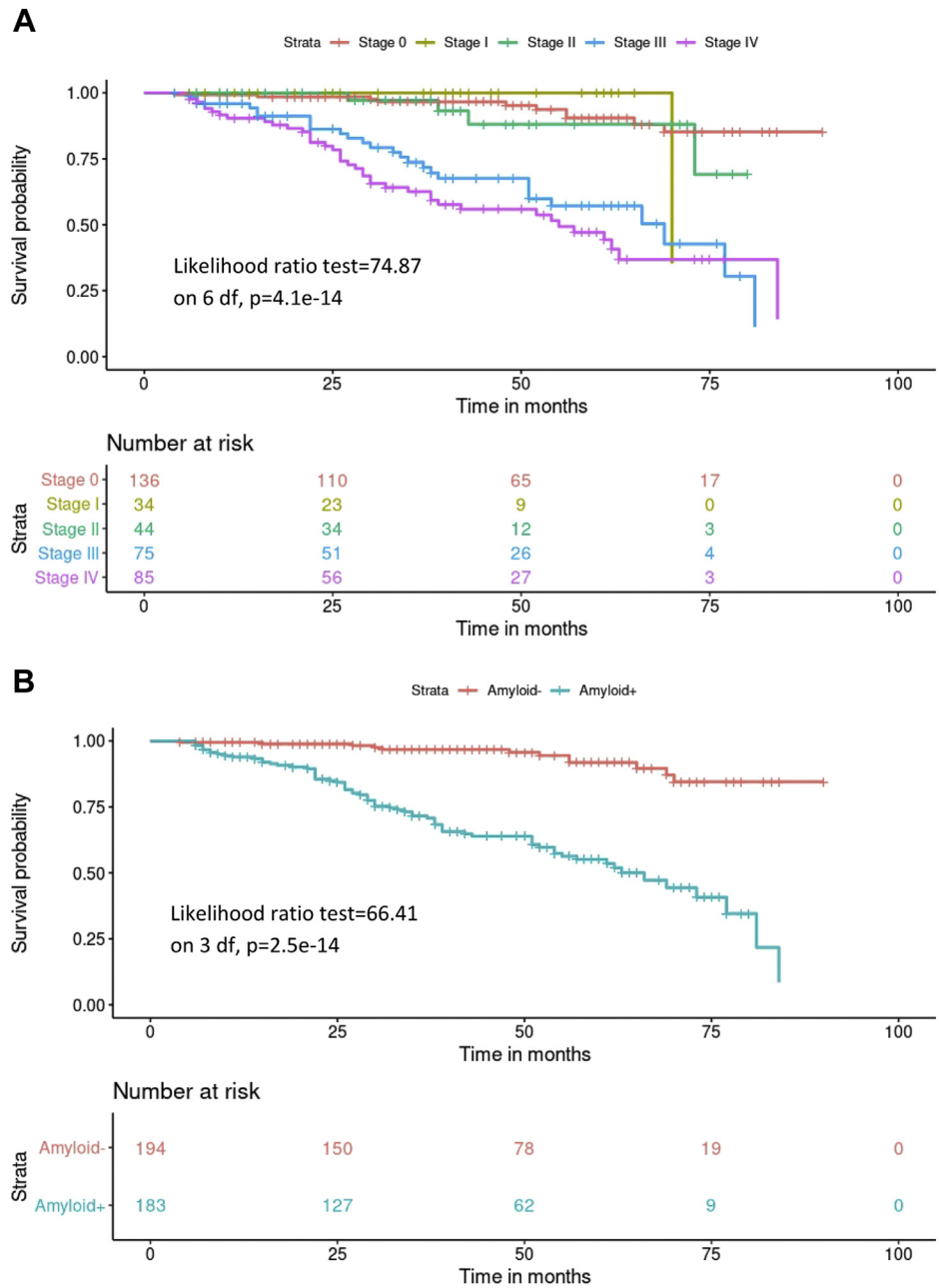

Fig. 2. Survival curves for amyloid in the ADNI-A sample, adjusted for age and sex. Survival curves comparing time to conversion of amyloid stages strata (A) versus global amyloid load (B) in the ADNI-A MCI sample. Curves were adjusted for the average age and sex distribution within each amyloid stratum. Abbreviations: ADNI, Alzheimer's Disease Neuroimaging Initiative; MCI, mild cognitive impairment.

with limited evidence for predicting conversion of healthy controls to MCI using ^{18}F tracers. Here, we used change in functional status as outcome, that is, from CDR score 0 to CDR score $\geq$0.5, and from CDR score 0.5 to CDR score $\geq$1. The global CDR score provides a commonly defined operationalized standard for functional assessment with high reliability across different cohorts (Schafer et al., 2004) and raters (Burke et al., 1988). In addition, the CDR is being used as primary or secondary outcome in ongoing clinical trials on AD. Diagnosis of MCI and dementia is closely linked with functional assessment using the CDR score (Woolf et al., 2016).

From a clinical perspective, the most interesting finding is the added value of regional amyloid stages over global amyloid status to identify a subsample of people with a very high risk of conversion. Thus, amyloid stage IV MCI cases had a 47% rate of conversion to dementia compared with 38% of the global amyloid-positive MCI cases in the ADNI-A sample, and in the INSIGHT-preAD cohort, 22% of the stage III/IV individuals with SMC converted to CDR 0.5 or higher compared with only 14% in the global amyloid-positive cases. The effects were similar in the ADNI-B MCI sample. Assessment of the model fit using AIC as fit criterion that penalizes for the higher number of parameters (Burnham and Anderson, 2004) with the amyloid staging compared with the binary global amyloid status supports the notion that the staging model would be preferred over the binary model in almost all cohorts and diagnostic subgroups except for the ADNI-B controls. In consequence, regional amyloid staging would allow identifying a high-risk group of preclinical or prodromal cases for future amyloid targeted treatment studies. This would require a larger screening effort as for example only 7% of

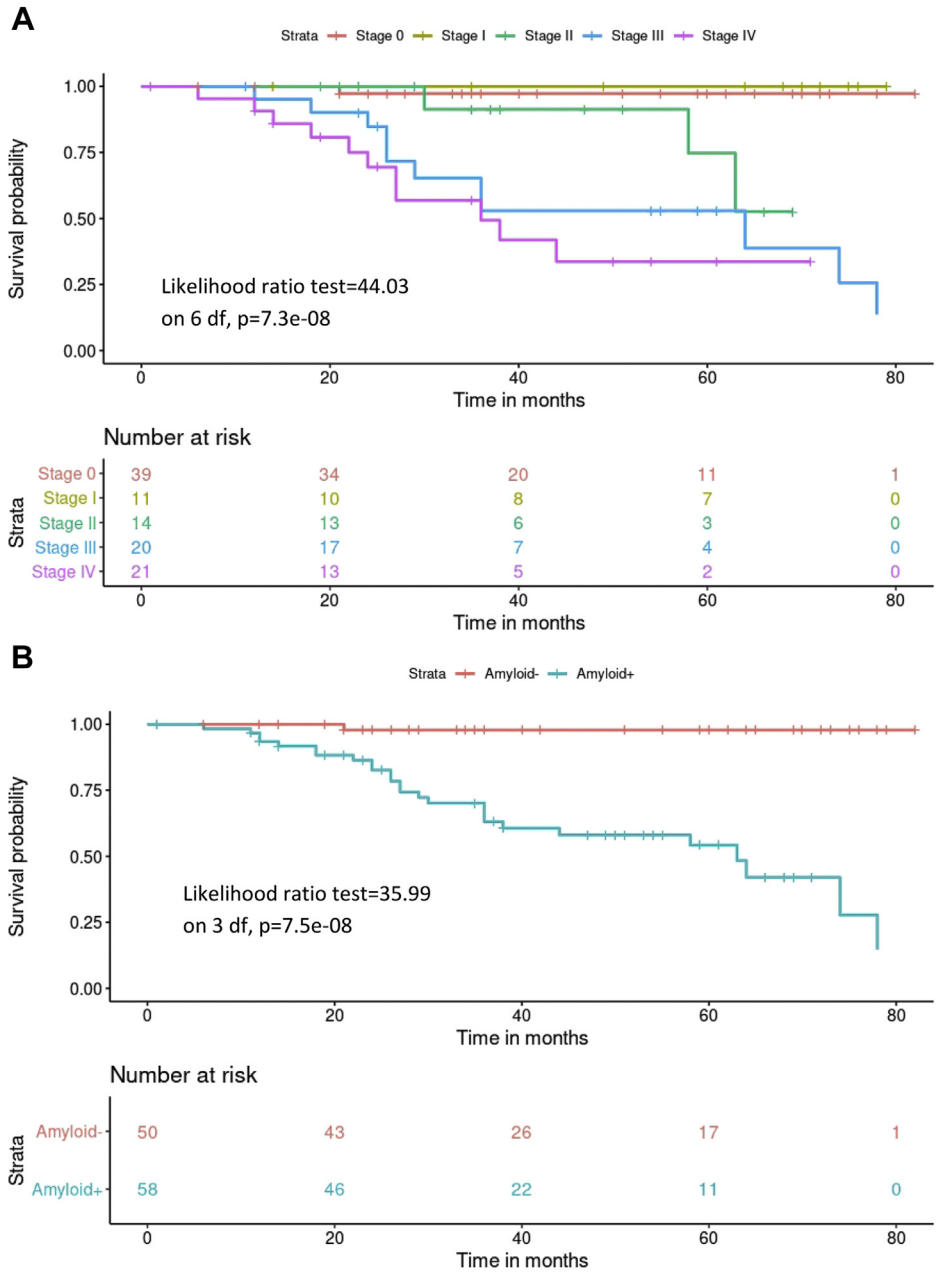

Fig. 3. Survival curves for amyloid in the ADNI-B sample, adjusted for age and sex. Cumulative survival of CDR conversion endpoint versus censoring comparing amyloid stages (A) versus global amyloid load (B) in the ADNI-B MCI sample. Curves were adjusted for the average age and sex distribution within each amyloid stratum. Abbreviations: ADNI, Alzheimer's Disease Neuroimaging Initiative; CDR, clinical dementia rating scale; MCI, mild cognitive impairment.

controls and 23% of MCI cases in the ADNI-A sample were in amyloid stage IV, compared with 23% global amyloid-positive controls and 49% global amyloid-positive MCI cases. However, a larger effort in screening is less costly than including people with a low risk of conversion. For example, at an initial conversion rate of 47% for stage IV MCI cases, one would need 429 cases to detect a 20% reduction of conversion rate at a level of significance of 5% with 80% power. However, at an initial conversion rate of 38% for global amyloid-positive MCI, this number would increase to 607 cases (Chow et al., 2008).[1]

In an alternative approach, global amyloid SUVR has been classified according to tertiles, where MCI cases in the highest tertile of global SUVR values had the highest HR for conversion (HR 9.4) (Jun et al., 2019), similar to the HRs of the regional stage III and IV MCI cases in our ADNI-A and ADNI-B samples. Both approaches are similarly easy to apply. However, the usefulness of the tertile staging scheme for predicting functional decline in cognitively healthy people and SMC cases has not been assessed so far. Another approach used an a priori distinction between neocortical and striatal amyloid deposition to define three stages based on (1) overall low amyloid, (2) high cortical but low striatal amyloid, and (3) high cortical and high striatal amyloid load (Hanseeuw et al., 2018). They found a significant association of these stages with

[1] Using the formula from Chow, S., Shao, J., Wang, H., 2008. Sample Size Calculations in Clinical Research, 2nd ed. Chapman & Hall/., page 89, implemented in http://powerandsamplesize.com/Calculators/Compare-2-Proportions/2-Sample-Equality (last access 8/2019).

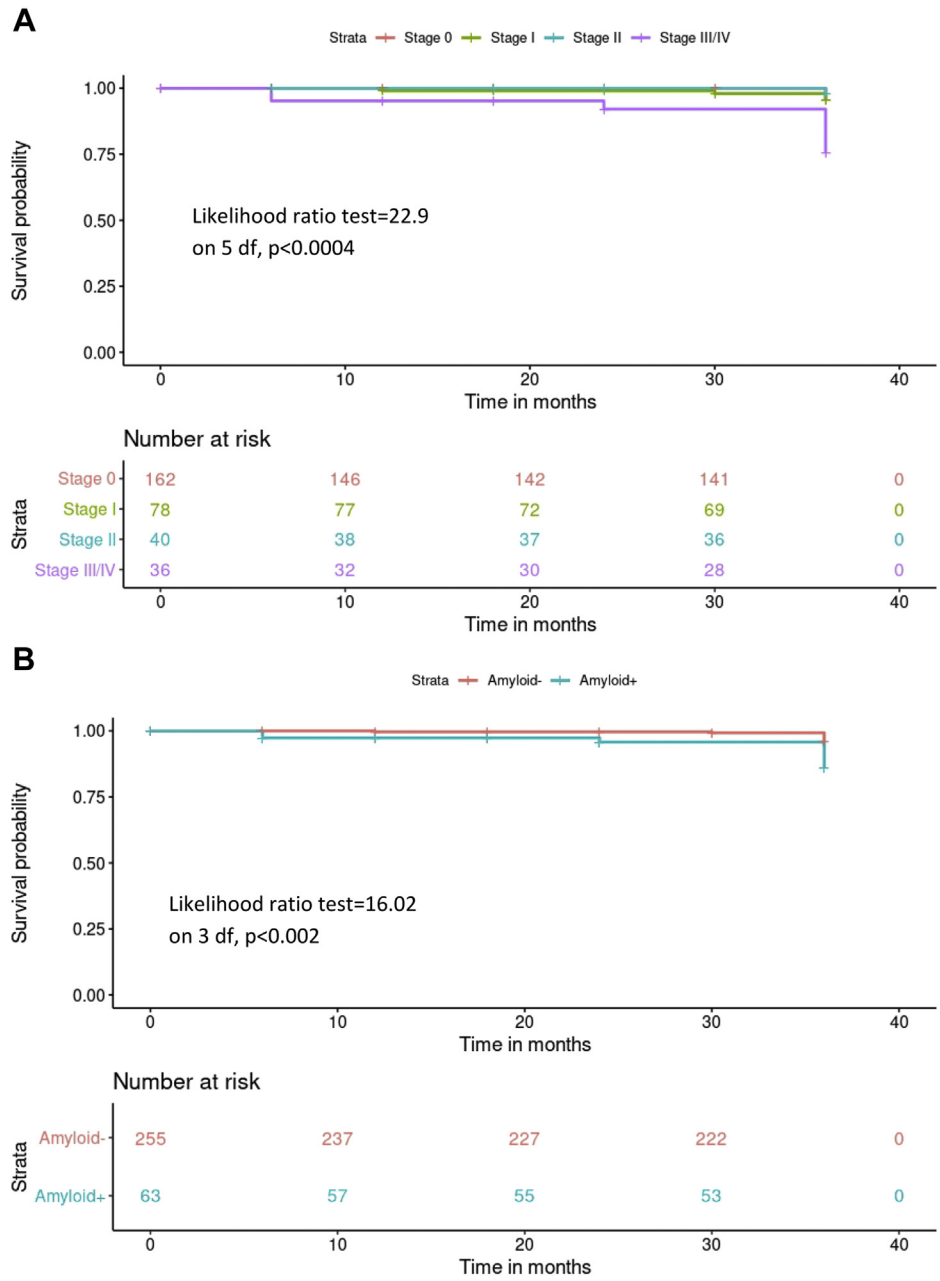

Fig. 4. Survival curves for amyloid in the INSIGHT-preAD sample, adjusted for age and sex. Cumulative survival of CDR conversion endpoint versus censoring comparing amyloid stages (A) versus global amyloid load (B) in the INSIGHT-preAD sample. Curves were adjusted for the average age and sex distribution within each amyloid stratum. Abbreviations: ADNI, Alzheimer's Disease Neuroimaging Initiative; CDR, clinical dementia rating scale; MCI, mild cognitive impairment.

rates of cognitive decline, with striatum amyloid load adding to the cortical amyloid load alone. We further extend this previous evidence for significant risk enrichment in advanced stages of amyloid progression by assessing the stage-specific risk of functional conversion and comparing it to more fine-grained stages of differential cortical involvement as well as to standard global amyloid status. Also, a recent staging scheme based on frequency of longitudinal regional involvement showed higher rates of cognitive decline with more advanced amyloid stages (Mattsson et al., 2019), but did not assess prediction of functional conversion. One can assume that stratification of global amyloid not only in two but in a higher number of classes will lead to more precise prediction of functional conversion as well. This is comparable with a top-down approach, where driven by the precision of prediction, a range of global thresholds would be defined. Here, we used a bottom-up approach with regional staging that was motivated by the notion of a consistent distribution of amyloid across cortical regions and compared its ability to predict functional conversion with the current standard of binarized global amyloid levels. For both ADNI and INSIGHT-preAD the more lenient cutoff yielded consistently lower performance so that we only reported the analysis results for the higher cutoff. In clinical practice, however, often not binarized amyloid levels are being used but expert visual reads of PET scans. A comparison with this clinical standard, however, was beyond the scope of the present study. One potential disadvantage of the method is the occurrence of mismatch cases that do not fit with the

staging scheme. In the current analysis, only 17 of 1202 cases did not match the regional staging scheme.

Our study presents some caveats. First, even when using regional amyloid stages, prediction accuracy falls short of a useful biomarker for individual counseling. Rather, regional amyloid stages seem useful as marker for risk enrichment of study samples at a group level. The use of regional amyloid stages to predict an individual's cognitive decline will likely need combination with markers of tau pathology, such as CSF p-tau concentration or Tau PET, or markers of neuronal degeneration, such as FDG PET or MRI volumetry. Second, the numbers of MCI and SMC cases in stages III and IV are substantial across the three cohorts, but for controls numbers are small so that inference for the controls is based on a small number of conversion events. However, the consistency of findings across the independent cohorts lends some credibility to the results. Third, we want to avoid the impression that the current data on the amyloid stages somehow prove a regional spread of amyloid through the brain. It is an intriguing observation that the large majority of cases with higher stage positive regions have also lower stages positive regions, but not the other way round, with only 17 of 1202 cases deviating from this pattern. This does, however, not prove a longitudinal spread of amyloid through the brain but would only conceptually fit to such assumption. Fourth, on a methodological note, here we used a constant threshold for determining regional amyloid positivity as previously defined (Grothe et al., 2017). As an alternative approach, one could define region-specific cutoffs that may better account for regionally differing noise levels and signal confounds in the amyloid-PET data. For example, subcortical nuclei such as the striatum that are entirely embedded in the white matter may be differentially affected by spill-in effects from the typically high nonspecific white matter signal compared with neocortical areas (Matsubara et al., 2016). We partially addressed this confound by using a 3-compartmental PVE correction method (Gonzalez-Escamilla et al., 2017), but this technique would not account for intrinsic differences in regional noise levels, such as signal confounds from traversing white matter bundles within the striatum itself. We work in parallel on a region-specific threshold approach but decided to use the constant threshold approach here, as it provided robust findings across two different cohorts in our previous analyses (Grothe et al., 2017; Sakr et al., 2019) and may be more easily applicable in future routine use. Still, a comparison of predictive accuracy of regional staging using constant versus region-specific thresholds is currently lacking.

In summary, we found that regional amyloid stages led to identify a high-risk group of controls, SMC, and MCI cases for subsequent functional decline. This finding may be useful for future clinical trials on amyloid targeted interventions to enrich the risk of conversion. Future studies are needed to explicitly model a direct versus an indirect effect of amyloid stages on cognitive decline via supposedly downstream markers such as regional hypometabolism or atrophy.

Disclosure statement

SJT participated in scientific advisory boards of Roche Pharma AG and MSD, and received lecture fees from Roche and MSD. MJG, FS, EC, PAC, IJ, and PL declare no conflict of interest. MOH received consultant fees from Blue Earth, and honoraria from Lilly, PIRAMAL, and GE as a speaker. SL received lecture honoraria from Roche and Servier. AV is an employee of Eisai Inc. Before November 2019 he had received lecture honoraria from Meg-Q, Roche, and Servier. BD received consultant fees from Lilly, Boehringer Ingelheim, and has received grants from Roche for his institution.

HH is an employee of Eisai Inc. and serves as Senior Associate Editor for the Journal Alzheimer's & Dementia; he does not receive any fees or honoraria since May 2019; before May 2019 he had received lecture fees from Servier, Biogen, and Roche, research grants from Pfizer, Avid, and MSD Avenir (paid to the institution), travel funding from Functional Neuromodulation, Axovant, Eli Lilly and company, Takeda and Zinfandel, GE Healthcare and Oryzon Genomics, consultancy fees from Qynapse, Jung Diagnostics, Cytox Ltd., Axovant, Anavex, Takeda and Zinfandel, GE Healthcare and Oryzon Genomics, and Functional Neuromodulation, and participated in scientific advisory boards of Functional Neuromodulation, Axovant, Eisai, Eli Lilly and company, Cytox Ltd., GE Healthcare, Takeda and Zinfandel, Oryzon Genomics and Roche Diagnostics.

HH is co-inventor in the following patents as a scientific expert and has received no royalties:

- *In Vitro* Multiparameter Determination Method for The Diagnosis and Early Diagnosis of Neurodegenerative Disorders Patent Number: 8916388.
- *In Vitro* Procedure for Diagnosis and Early Diagnosis of Neurodegenerative Diseases Patent Number: 8298784.
- Neurodegenerative Markers for Psychiatric Conditions Publication Number: 20120196300.
- *In Vitro* Multiparameter Determination Method for The Diagnosis and Early Diagnosis of Neurodegenerative Disorders Publication Number: 20100062463.
- *In Vitro* Method for The Diagnosis and Early Diagnosis of Neurodegenerative Disorders Publication Number: 20100035286.
- *In Vitro* Procedure for Diagnosis and Early Diagnosis of Neurodegenerative Diseases Publication Number: 20090263822.
- *In Vitro* Method for The Diagnosis of Neurodegenerative Diseases Patent Number: 7547553.
- CSF Diagnostic in Vitro Method for Diagnosis of Dementias and Neuroinflammatory Diseases Publication Number: 20080206797.
- *In Vitro* Method for The Diagnosis of Neurodegenerative Diseases Publication Number: 20080199966.
- Neurodegenerative Markers for Psychiatric Conditions Publication Number: 20080131921.

CRediT authorship contribution statement

Stefan J. Teipel: Conceptualization, Formal analysis, Writing - original draft, Writing - review & editing. **Martin Dyrba:** Software, Formal analysis, Data curation, Visualization. **Patrizia A. Chiesa:** Resources, Data curation, Writing - original draft. **Fatemah Sakr:** Writing - original draft, Writing - review & editing. **Irina Jelistratova:** Formal analysis, Writing - original draft. **Simone Lista:** Resources, Writing - original draft, Investigation. **Andrea Vergallo:** Resources, Writing - original draft, Investigation. **Pablo Lemercier:** Formal analysis, Software. **Enrica Cavedo:** Resources, Data curation, Writing - original draft. **Marie Odile Habert:** Resources, Investigation, Writing - original draft. **Bruno Dubois:** Supervision, Investigation, Writing - review & editing. **Harald Hampel:** Supervision, Writing - review & editing. **Michel J. Grothe:** Conceptualization, Writing - original draft, Writing - review & editing.

Acknowledgements

ADNI cohort: Data collection and sharing for this project was funded by the Alzheimer's Disease Neuroimaging Initiative (ADNI) (National Institutes of Health Grant U01 AG024904) and DOD

ADNI (Department of Defense award number W81XWH-12-2–0012). ADNI is funded by the National Institute on Aging, the National Institute of Biomedical Imaging and Bioengineering, and through generous contributions from the following: Alzheimer's Association; Alzheimer's Drug Discovery Foundation; Araclon Biotech; BioClinica, Inc.; Biogen Idec Inc.; Bristol-Myers Squibb Company; Eisai Inc.; Elan Pharmaceuticals, Inc.; Eli Lilly and Company; EuroImmun; F. Hoffmann-La Roche Ltd and its affiliated company Genentech, Inc.; Fujirebio; GE Healthcare; IXICO Ltd.; Janssen Alzheimer Immunotherapy Research & Development, LLC.; Johnson & Johnson Pharmaceutical Research & Development LLC.; Medpace, Inc.; Merck & Co., Inc.; Meso Scale Diagnostics, LLC.; NeuroRx Research; Neurotrack Technologies; Novartis Pharmaceuticals Corporation; Pfizer Inc.; Piramal Imaging; Servier; Synarc Inc.; and Takeda Pharmaceutical Company. The Canadian Institutes of Health Research is providing funds to support ADNI clinical sites in Canada. Private sector contributions are facilitated by the Foundation for the National Institutes of Health (www.fnih.org). The grantee organization is the Northern California Institute for Research and Education, and the study is coordinated by the Alzheimer's Disease Cooperative Study at the University of California, San Diego. ADNI data are disseminated by the Laboratory for Neuro Imaging at the University of Southern California.

This research and this manuscript was part of the translational research Program "PHOENIX", awarded to HH, and administered by the Sorbonne University Foundation and sponsored by la *Fondation pour la Recherche sur Alzheimer*.

INSIGHT-preAD cohort: The study was promoted by INSERM in collaboration with ICM, IHU-A-ICM and Pfizer and has received support within the "Investissement d'Avenir" (ANR-10-AIHU-06) French program. The study was promoted in collaboration with the "CHU de Bordeaux" (coordination CIC EC7), the promoter of Memento cohort, funded by the Foundation Plan-Alzheimer. The study was further supported by AVID/Lilly.

CATI is a French neuroimaging platform funded by the French Plan Alzheimer (available at http://cati-neuroimaging.com).

INSIGHT-preAD study group: Hovagim Bakardjian, Habib Benali, Hugo Bertin, Joel Bonheur, Laurie Boukadida, Nadia Boukerrou, Enrica Cavedo, Patrizia A. Chiesa, Olivier Colliot, Bruno Dubois, Marion Dubois, Stéphane Epelbaum, Geoffroy Gagliardi, Remy Genthon, Marie-Odile Habert, Harald Hampel, Marion Houot, Aurélie Kas, Foudil Lamari, Marcel Levy, Simone Lista, Christiane Metzinger, Fanny Mochel, Francis Nyasse, Catherine Poisson, Marie-Claude Potier, Marie Revillon, Antonio Santos, Katia Santos Andrade, Marine Sole, Mohmed Surtee, Michel Thiebaut de Schotten, Andrea Vergallo, Nadjia Younsi.

HH is an employee of Eisai Inc. This work has been performed during his previous position at Sorbonne University, Paris, France. At Sorbonne University he was supported by the AXA Research Fund, the "*Fondation partenariale Sorbonne Université*" and the "*Fondation pour la Recherche sur Alzheimer*", Paris, France. AV is an employee of Eisai Inc. This work has been performed during his previous position at Sorbonne University, Paris, France.

MJG is supported by the "Miguel Servet" program [CP19/00031] of the Spanish Instituto de Salud Carlos III (ISCIIIFEDER).

Appendix A. Supplementary data

Supplementary data associated with this article can be found, in the online version, at https://doi.org/10.1016/j.neurobiolaging.2020.03.011.

References

Baker, J.E., Lim, Y.Y., Pietrzak, R.H., Hassenstab, J., Snyder, P.J., Masters, C.L., Maruff, P., 2017. Cognitive impairment and decline in cognitively normal older adults with high amyloid-beta: a meta-analysis. Alzheimers Dement. 6, 108–121.

Berg, L., 1988. Clinical dementia rating (CDR). Psychopharmacol. Bull. 24, 637–639.

Burke, W.J., Miller, J.P., Rubin, E.H., Morris, J.C., Coben, L.A., Duchek, J., Wittels, I.G., Berg, L., 1988. Reliability of the Washington university clinical dementia rating. Arch. Neurol. 45, 31–32.

Burnham, K.P., Anderson, D.R., 2004. Multimodel inference–understanding AIC and BIC in model selection. Sociol. Method Res. 33, 261–304.

Catafau, A.M., Bullich, S., Seibyl, J.P., Barthel, H., Ghetti, B., Leverenz, J., Ironside, J.W., Schulz-Schaeffer, W.J., Hoffmann, A., Sabri, O., 2016. Cerebellar amyloid-beta plaques: how frequent are they, and do they influence 18F-florbetaben SUV ratios? J. Nucl. Med. 57, 1740–1745.

Chen, X., Li, M., Wang, S., Zhu, H., Xiong, Y., Liu, X., 2014. Pittsburgh compound B retention and progression of cognitive status–a meta-analysis. Eur. J. Neurol. 21, 1060–1067.

Cho, S.H., Shin, J.H., Jang, H., Park, S., Kim, H.J., Kim, S.E., Kim, S.J., Kim, Y., Lee, J.S., Na, D.L., Lockhart, S.N., Rabinovici, G.D., Seong, J.K., Seo, S.W., Alzheimer's Disease Neuroimaging, I., 2018. Amyloid involvement in subcortical regions predicts cognitive decline. Eur. J. Nucl. Med. Mol. Imaging 45, 2368–2376.

Chow, S., Shao, J., Wang, H., 2008. Sample Size Calculations in Clinical Research, 2nd ed. Chapman & Hall, Boca Raton, FL.

Clark, C.M., Pontecorvo, M.J., Beach, T.G., Bedell, B.J., Coleman, R.E., Doraiswamy, P.M., Fleisher, A.S., Reiman, E.M., Sabbagh, M.N., Sadowsky, C.H., Schneider, J.A., Arora, A., Carpenter, A.P., Flitter, M.L., Joshi, A.D., Krautkramer, M.J., Lu, M., Mintun, M.A., Skovronsky, D.M., Group, A.-A.S., 2012. Cerebral PET with florbetapir compared with neuropathology at autopsy for detection of neuritic amyloid-beta plaques: a prospective cohort study. Lancet Neurol. 11, 669–678.

Clark, C.M., Schneider, J.A., Bedell, B.J., Beach, T.G., Bilker, W.B., Mintun, M.A., Pontecorvo, M.J., Hefti, F., Carpenter, A.P., Flitter, M.L., Krautkramer, M.J., Kung, H.F., Coleman, R.E., Doraiswamy, P.M., Fleisher, A.S., Sabbagh, M.N., Sadowsky, C.H., Reiman, E.P., Zehntner, S.P., Skovronsky, D.M., 2011a. Use of florbetapir-PET for imaging beta-amyloid pathology. JAMA 305, 275–283.

Desikan, R.S., Segonne, F., Fischl, B., Quinn, B.T., Dickerson, B.C., Blacker, D., Buckner, R.L., Dale, A.M., Maguire, R.P., Hyman, B.T., Albert, M.S., Killiany, R.J., 2006. An automated labeling system for subdividing the human cerebral cortex on MRI scans into gyral based regions of interest. NeuroImage 31, 968–980.

Dubois, B., Epelbaum, S., Nyasse, F., Bakardjian, H., Gagliardi, G., Uspenskaya, O., Houot, M., Lista, S., Cacciamani, F., Potier, M.C., Bertrand, A., Lamari, F., Benali, H., Mangin, J.F., Colliot, O., Genthon, R., Habert, M.O., Hampel, H., Group, I.N.-p.s., 2018. Cognitive and neuroimaging features and brain beta-amyloidosis in individuals at risk of Alzheimer's disease (INSIGHT-preAD): a longitudinal observational study. Lancet Neurol. 17, 335–346.

Fleisher, A.S., Chen, K., Liu, X., Roontiva, A., Thiyyagura, P., Ayutyanont, N., Joshi, A.D., Clark, C.M., Mintun, M.A., Pontecorvo, M.J., Doraiswamy, P.M., Johnson, K.A., Skovronsky, D.M., Reiman, E.M., 2011. Using positron emission tomography and florbetapir F18 to image cortical amyloid in patients with mild cognitive impairment or dementia due to Alzheimer disease. Arch. Neurol. 68, 1404–1411.

Folstein, M.F., Folstein, S.E., McHugh, P.R., 1975. Mini-mental-state: a practical method for grading the cognitive state of patients for the clinician. J. Psychiatr. Res. 12, 189–198.

Frings, L., Hellwig, S., Bormann, T., Spehl, T.S., Buchert, R., Meyer, P.T., 2018. Amyloid load but not regional glucose metabolism predicts conversion to Alzheimer's dementia in a memory clinic population. Eur. J. Nucl. Med. Mol. Imaging 45, 1442–1448.

Gonzalez-Escamilla, G., Lange, C., Teipel, S., Buchert, R., Grothe, M.J., Alzheimer's Disease Neuroimaging, I., 2017. PETPVE12: an SPM toolbox for Partial Volume Effects correction in brain PET–application to amyloid imaging with AV45-PET. NeuroImage 147, 669–677.

Grothe, M.J., Barthel, H., Sepulcre, J., Dyrba, M., Sabri, O., Teipel, S.J., Alzheimer's Disease Neuroimaging, I., 2017. In vivo staging of regional amyloid deposition. Neurology 89, 2031–2038.

Habert, M.O., Bertin, H., Labit, M., Diallo, M., Marie, S., Martineau, K., Kas, A., Causse-Lemercier, V., Bakardjian, H., Epelbaum, S., Chetelat, G., Houot, M., Hampel, H., Dubois, B., Mangin, J.F., Group, I.-A.s., 2018. Evaluation of amyloid status in a cohort of elderly individuals with memory complaints: validation of the method of quantification and determination of positivity thresholds. Ann. Nucl. Med. 32, 75–86.

Hanseeuw, B.J., Betensky, R.A., Mormino, E.C., Schultz, A.P., Sepulcre, J., Becker, J.A., Jacobs, H.I.L., Buckley, R.F., LaPoint, M.R., Vannini, P., Donovan, N.J., Chhatwal, J.P., Marshall, G.A., Papp, K.V., Amariglio, R.E., Rentz, D.M., Sperling, R.A., Johnson, K.A., Alzheimer's Disease Neuroimaging, I., Harvard Aging Brain, S., 2018. PET staging of amyloidosis using striatum. Alzheimers Dement. 14, 1281–1292.

Iaccarino, L., Chiotis, K., Alongi, P., Almkvist, O., Wall, A., Cerami, C., Bettinardi, V., Gianolli, L., Nordberg, A., Perani, D., 2017. A cross-validation of FDG- and amyloid-PET biomarkers in mild cognitive impairment for the risk prediction to dementia due to alzheimer's disease in a clinical setting. J. Alzheimers Dis. 59, 603–614.

Joshi, A.D., Pontecorvo, M.J., Clark, C.M., Carpenter, A.P., Jennings, D.L., Sadowsky, C.H., Adler, L.P., Kovnat, K.D., Seibyl, J.P., Arora, A., Saha, K., Burns, J.D.,

Lowrey, M.J., Mintun, M.A., Skovronsky, D.M., Florbetapir, F.S.I., 2012. Performance characteristics of amyloid PET with florbetapir F 18 in patients with alzheimer's disease and cognitively normal subjects. J. Nucl. Med. 53, 378–384.
Jun, S., Kim, H., Kim, B.S., Yoo, B.G., Lee, W.G., Alzheimer's Disease Neuroimaging, I., 2019. Quantitative brain amyloid measures predict time-to-progression from amnestic mild cognitive impairment to alzheimer's disease. J. Alzheimers Dis. 70, 477–486.
Klunk, W.E., Koeppe, R.A., Price, J.C., Benzinger, T.L., Devous, M.D., Sr, Jagust, W.J., Johnson, K.A., Mathis, C.A., Minhas, D., Pontecorvo, M.J., Rowe, C.C., Skovronsky, D.M., Mintun, M.A., 2015. The Centiloid Project: standardizing quantitative amyloid plaque estimation by PET. Alzheimers Dement. 11, 1–15.e11-14.
Landau, S.M., Breault, C., Joshi, A.D., Pontecorvo, M., Mathis, C.A., Jagust, W.J., Mintun, M.A., Alzheimer's Disease Neuroimaging, I., 2013. Amyloid-beta imaging with Pittsburgh compound B and florbetapir: comparing radiotracers and quantification methods. J. Nucl. Med. 54, 70–77.
Martinez, G., Vernooij, R.W., Fuentes Padilla, P., Zamora, J., Flicker, L., Bonfill Cosp, X., 2017. 18F PET with florbetaben for the early diagnosis of Alzheimer's disease dementia and other dementias in people with mild cognitive impairment (MCI). Cochrane Database Syst. Rev. 11, CD012883.
Matsubara, K., Ibaraki, M., Shimada, H., Ikoma, Y., Suhara, T., Kinoshita, T., Ito, H., 2016. Impact of spillover from white matter by partial volume effect on quantification of amyloid deposition with [(11)C]PiB PET. NeuroImage 143, 316–324.
Mattsson, N., Palmqvist, S., Stomrud, E., Vogel, J., Hansson, O., 2019. Staging beta-amyloid pathology with amyloid positron emission tomography. JAMA Neurol. e1–e11.
Morris, J.C., Roe, C.M., Grant, E.A., Head, D., Storandt, M., Goate, A.M., Fagan, A.M., Holtzman, D.M., Mintun, M.A., 2009. Pittsburgh compound B imaging and prediction of progression from cognitive normality to symptomatic Alzheimer disease. Arch. Neurol. 66, 1469–1475.
Müller-Gärtner, H.W., Links, J.M., Prince, J.L., Bryan, R.N., McVeigh, E., Leal, J.P., Davatzikos, C., Frost, J.J., 1992. Measurement of radiotracer concentration in brain gray matter using positron emission tomography: MRI-based correction for partial volume effects. J. Cerbral Blood Flow Metab. 12, 571–583.
Quigley, H., Colloby, S.J., O'Brien, J.T., 2011. PET imaging of brain amyloid in dementia: a review. Int. J. Geriatr. Psychiatry 26, 991–999.
Risacher, S.L., Kim, S., Nho, K., Foroud, T., Shen, L., Petersen, R.C., Jack Jr., C.R., Beckett, L.A., Aisen, P.S., Koeppe, R.A., Jagust, W.J., Shaw, L.M., Trojanowski, J.Q., Weiner, M.W., Saykin, A.J., Alzheimer's Disease Neuroimaging, I., 2015. APOE effect on Alzheimer's disease biomarkers in older adults with significant memory concern. Alzheimers Dement. 11, 1417–1429.
Sakr, F.A., Grothe, M.J., Cavedo, E., Jelistratova, I., Habert, M.O., Dyrba, M., Gonzalez-Escamilla, G., Bertin, H., Locatelli, M., Lehericy, S., Teipel, S., Dubois, B., Hampel, H., for the, I.-p.s.g., Alzheimer Precision Medicine, I., 2019. Applicability of in vivo staging of regional amyloid burden in a cognitively normal cohort with subjective memory complaints: the INSIGHT-preAD study. Alzheimers Res. Ther. 11, 15.
Schafer, K.A., Tractenberg, R.E., Sano, M., Mackell, J.A., Thomas, R.G., Gamst, A., Thal, L.J., Morris, J.C., Alzheimer's Disease Cooperative, S., 2004. Reliability of monitoring the clinical dementia rating in multicenter clinical trials. Alzheimer Dis. Assoc. Disord. 18, 219–222.
Schreiber, S., Landau, S.M., Fero, A., Schreiber, F., Jagust, W.J., Alzheimer's Disease Neuroimaging, I., 2015. Comparison of visual and quantitative florbetapir F 18 positron emission tomography analysis in predicting mild cognitive impairment outcomes. JAMA Neurol. 72, 1183–1190.
Thal, D.R., Capetillo-Zarate, E., Del Tredici, K., Braak, H., 2006. The development of amyloid beta protein deposits in the aged brain. Sci. Aging Knowledge Environ. 2006, re1.
Villemagne, V.L., Pike, K.E., Chetelat, G., Ellis, K.A., Mulligan, R.S., Bourgeat, P., Ackermann, U., Jones, G., Szoeke, C., Salvado, O., Martins, R., O'Keefe, G., Mathis, C.A., Klunk, W.E., Ames, D., Masters, C.L., Rowe, C.C., 2011. Longitudinal assessment of Abeta and cognition in aging and Alzheimer disease. Ann. Neurol. 69, 181–192.
Woolf, C., Slavin, M.J., Draper, B., Thomassen, F., Kochan, N.A., Reppermund, S., Crawford, J.D., Trollor, J.N., Brodaty, H., Sachdev, P.S., 2016. Can the clinical dementia rating scale identify mild cognitive impairment and predict cognitive and functional decline? Dement. Geriatr. Cogn. Disord. 41, 292–302.
Zhang, S., Smailagic, N., Hyde, C., Noel-Storr, A.H., Takwoingi, Y., McShane, R., Feng, J., 2014. (11)C-PIB-PET for the early diagnosis of Alzheimer's disease dementia and other dementias in people with mild cognitive impairment (MCI). Cochrane Database Syst. Rev. 7, CD010386.